



2 Deformation of Mexico from continuous GPS from 1993 3 to 2008

4 **B. Marquez-Azua**

5 *DGOT, SisVoc, Universidad de Guadalajara, Avenida Maestros y Mariano Barcenas, 93106, Guadalajara, Jalisco,*
6 *Mexico*

7 **C. DeMets**

8 *Department of Geology and Geophysics, University of Wisconsin-Madison, 1215 Dayton, Madison, Wisconsin 53706,*
9 *USA (chuck@geology.wisc.edu)*

10 [1] We combine the velocities of 13 continuous Global Positioning System stations from Mexico and 448
11 North American plate stations to better understand deformation and earthquake cycle effects in Mexico.
12 Velocities estimated at the Mexican sites from high-quality GPS data collected since 2003 show no
13 evidence for a previously reported eastward bias at sites in and near the Yucatan peninsula. The new
14 velocities are compared to the predictions of two models, one in which all motion in Mexico is attributed to
15 North American plate motion and the second of which attributes site motions to a combination of plate
16 motion and the elastic effects of frictional coupling along the Mexican subduction zone and faults in the
17 Gulf of California. The second model fits the velocities within their estimated uncertainties. Mainland
18 Mexico thus moves with the North American plate to within 1 mm per year and undergoes elastic
19 interseismic deformation far into its interior. Two stations inland from the Guerrero and Oaxaca segments
20 of the Mexican subduction zone have alternated between several-year-long periods of landward motion
21 and several-month-long periods of trenchward motion frequently since 1993, consistent with previously
22 described, repeating transient slip events along the subduction interface. The motions of two stations inland
23 from the Rivera plate subduction zone are dominated by the coseismic and postseismic effects of the $M =$
24 8.0 , 9 October 1995 Colima-Jalisco earthquake and $M = 7.5$, 22 January 2003 Tecoman earthquake
25 offshore from western Mexico.

26 **Components:** 8529 words, 8 figures, 2 tables.

27 **Keywords:** tectonics.

28 **Index Terms:** 1240 Geodesy and Gravity: Satellite geodesy: results (6929, 7215, 7230, 7240); 1207 Geodesy and Gravity:
29 Transient deformation (6924, 7230, 7240); 1209 Geodesy and Gravity: Tectonic deformation (6924).

30 **Received** 11 October 2008; **Revised** 2 December 2008; **Accepted** 22 December 2008; **Published** XX Month 2009.

31 Marquez-Azua, B., and C. DeMets (2009), Deformation of Mexico from continuous GPS from 1993 to 2008, *Geochem.*
32 *Geophys. Geosyst.*, 10, XXXXXX, doi:10.1029/2008GC002278.

34 1. Introduction

35 [2] Over the past decade, continuous and campaign
36 Global Positioning System (GPS) measurements in

Mexico have established an increasingly reliable 37
basis for addressing questions about deformation 38
within this tectonically active country. To date, 39
most GPS studies in Mexico have focused on 40

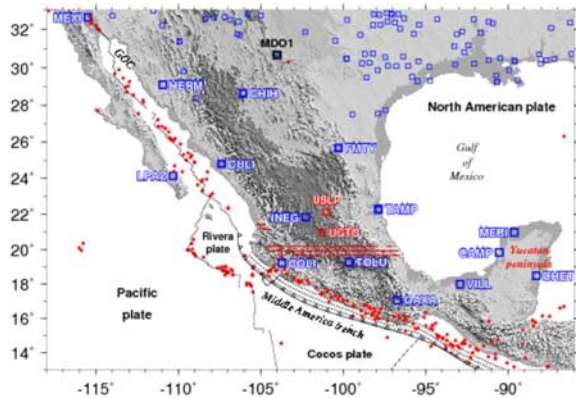


Figure 1. Tectonic setting, seismicity, topography, and location map for the study area. Red circles show epicenters of all 1963–2008 earthquakes with magnitudes greater than 5.5 and depths above 40 km and are from the U.S. Geological Survey National Earthquake Information Center files. Labeled blue squares specify locations and names of the 15 continuous RGNA GPS stations that are the subject of this study. Smaller blue squares indicate the locations of other continuous GPS stations whose motions are used herein. Red squares and labels indicate recently installed RGNA sites not used for this analysis. Area indicated by horizontal red stripes is the Mexican volcanic belt. Open circles between trench and coast are surface-projected node locations that approximate locked areas of the subduction interface for elastic calculations described in text. “GOC” is Gulf of California.

41 regions located between the Pacific coast and
42 Mexican volcanic belt (Figure 1), where large-
43 magnitude earthquakes along the Mexican subduc-
44 tion zone pose a significant hazard. Such studies
45 have revealed significantly more complex earth-
46 quake cycle deformation than was imagined less
47 than a decade ago. In particular, GPS measure-
48 ments clearly establish that frequent transient, aseismic
49 slip occurs along the Guerrero and Oaxaca seg-
50 ments of the subduction interface, raising impor-
51 tant questions about whether such slip influences the timing
52 of large subduction zone earthquakes [Lowry *et al.*,
53 2001; Kostoglodov *et al.*, 2003; Yoshioka *et al.*,
54 2004; Franco *et al.*, 2005; Brudzinski *et al.*, 2007;
55 Larson *et al.*, 2007; Correa-Mora *et al.*, 2008;
56 F. Correa-Mora *et al.*, Transient deformation in
57 southern Mexico in 2006 and 2007: Evidence for
58 distinct deep-slip patches beneath Guerrero and
59 Oaxaca, submitted to, *Geochemistry, Geophysics,*
60 *Geosystems*, 2009].

61 [3] Complementing this work, questions about the
62 large-scale tectonics of Mexico are addressed by

Marquez-Azua and DeMets [2003] and *Marquez-* 63
Azua et al. [2004] using continuous GPS measure- 64
ments from a 15-station nationwide GPS network 65
that has been operated by the Mexican government 66
since 1993 (Figure 1). On the basis of non-P-code 67
GPS data that were collected prior to mid-2001, 68
Marquez-Azua and DeMets [2003, hereinafter re- 69
ferred to as MD2003] conclude that GPS stations 70
north of the Mexican Volcanic Belt move with the 71
North America plate within their 1–2 mm a⁻¹ 72
velocity uncertainties but that stations south of 73
the volcanic belt, most notably in the Yucatan 74
peninsula, move 1–4 mm a⁻¹ to the east relative 75
to the North American plate. MD2003 examine 76
whether this unexpected eastward motion could be 77
an artifact of the non-P-code GPS data that were 78
used to determine the station velocities or whether 79
any geologic evidence supports the slow eastward 80
movement of southern Mexico but find no com- 81
pelling evidence for either explanation. 82

[4] In this study, we use an additional 7 years of 83
continuous measurements from 13 of the 15 GPS 84
stations that were used by MD2003 to revisit 85
questions about the large-scale tectonics of main- 86
land Mexico. New data from the other two stations 87
used by MD2003, namely, LPAZ and MEXI in 88
Baja and Alta California, provide little information 89
relevant to this study and are not reported here 90
since the station velocities have not changed sub- 91
stantially. Critically, the new GPS data include 92
high-quality P-code and carrier phase data that 93
have been recorded continuously since early 94
2003. These data provide an independent test of 95
the accuracy of the MD2003 station velocities and 96
are used below to estimate a useful new upper 97
bound on possible motion across the Mexican 98
volcanic belt. The motions of four RGNA stations 99
that record coseismic, postseismic, interseismic, 100
and transient-slip processes caused by subduction 101
of the Rivera and Cocos plates constitute the 102
longest continuous records of earthquake cycle 103
deformation in Mexico and are presented and 104
described here for the first time for the benefit of 105
future investigators. 106

2. Tectonic Setting 107

[5] The active deformation of Mexico is caused 108
primarily by the interactions between five tectonic 109
plates that share boundaries within or near Mexico 110
(Figure 1). Along the Mexican segment of the 111
Middle America trench (Figure 1), the Rivera and 112
Cocos plates subduct at rates that increase from 113

t1.1 **Table 1.** RGNA Site Velocities in ITRF2005^a

t1.3	Site	Latitude °N	Longitude °W	Velocities		Correlation Coefficient
				$V_n \pm 1\sigma$	$V_e \pm 1\sigma$	
t1.4	CAMP	19.845	90.540	-0.5 ± 0.5	-8.1 ± 0.5	0.029
t1.5	CHET	18.495	88.299	0.4 ± 0.5	-7.4 ± 0.6	-0.166
t1.6	CHIH	28.662	106.087	-6.6 ± 0.5	-11.4 ± 0.6	-0.045
t1.7	COLI	19.244	103.702	–	–	–
t1.8	CULI	24.799	107.384	-6.9 ± 0.5	-9.3 ± 1.1	-0.156
t1.9	FMTY	25.715	100.313	-4.8 ± 0.6	-10.3 ± 0.6	-0.043
t1.10	HERM	29.093	110.967	-7.2 ± 0.5	-12.1 ± 0.6	-0.044
t1.11	INEG	21.856	102.284	-4.9 ± 0.5	-8.4 ± 0.7	0.060
t1.12	MERI	20.980	89.620	-0.1 ± 0.5	-8.5 ± 0.5	-0.022
t1.13	OAXA	17.078	96.717	0.8 ± 0.9	-2.9 ± 0.9	0.373
t1.14	TAMP	22.278	97.864	-4.5 ± 0.5	-9.0 ± 0.7	0.111
t1.15	TOLU	19.293	99.644	-2.0 ± 0.8	-5.3 ± 0.6	-0.008
t1.16	VILL	17.990	92.931	0.8 ± 0.5	-8.2 ± 0.6	-0.122

^aRGNA station locations and horizontal velocities. Best-fitting velocities are determined for the period 20 January 2003 to 1 August 2008. No velocity is given for site COLI, whose motion is dominated by the postseismic effects of the 22 January 2003 Tecoman earthquake. North and east velocity components are specified by V_n and V_e , respectively, and are in units of millimeters per year. Geodetic latitudes are specified.

114 $\sim 20 \text{ mm a}^{-1}$ at the northwestern end of the trench
 115 [DeMets and Wilson, 1997] to $\sim 80 \text{ mm a}^{-1}$ near
 116 the Mexico-Guatemala border [DeMets, 2001]. The
 117 elastic effects associated with this subduction have
 118 been measured hundreds of kilometers inland from
 119 the Pacific coast [Yoshioka et al., 2004; Correa-
 120 Mora et al., 2008] and dominate interseismic
 121 deformation in southern and western Mexico. In
 122 the Gulf of California (Figure 1), motion between
 123 the Pacific and North American plates is parti-
 124 tioned between faults in the gulf, which accommo-
 125 date $\sim 48 \text{ mm a}^{-1}$ of dextral strike-slip motion
 126 [DeMets, 1995], and faults within and west of the
 127 Baja California peninsula [Michaud et al., 2004],
 128 which accommodate an additional 3 to 5 mm a^{-1}
 129 of dextral slip [Dixon et al., 2000; Plattner et al.,
 130 2007]. In the state of Chiapas in southern Mexico,
 131 distributed faulting and folding occurs in response
 132 to motion between the Caribbean and North Amer-
 133 ican plates [Guzman-Speziale et al., 1989; Guzman-
 134 Speziale and Meneses-Rocha, 2000].

135 [6] The other major tectonic feature in Mexico is
 136 the Mexican Volcanic Belt, which extends $\sim 900 \text{ km}$
 137 across central Mexico (Figure 1) and poses signif-
 138 icant volcanic and seismic hazards to interior areas
 139 of the country. Recent structural studies of faults
 140 that displace Quaternary-age rocks in the central
 141 part of the volcanic belt suggest that the bulk
 142 Neogene motion across the volcanic belt has been
 143 limited to NNW–SSE-oriented extension of $0.2 \pm$
 144 0.05 mm a^{-1} [Suter et al., 2001; Langridge et al.,
 145 2000]. Similarly, the estimated Quaternary defor-
 146 mation rate across faults at the western end of the

volcanic belt is only 0.1 mm a^{-1} [Ferrari and
 Rosas-Elguera, 2000].

3. Data

[7] The primary data emphasized in this analysis
 are from the Red Geodesica Nacional Activa
 (RGNA), a continuous GPS network operated
 by the Mexican government agency Institutos
 Nacional Estadística y Geografía (INEGI). The
 RGNA network presently consists of 17 continu-
 ous GPS stations (Figure 1), of which 15 have
 operated continuously for more than a decade and
 are used for this analysis (Table 1) and two were
 added after 2007 (UGTO and USLP). Since mid-
 2004, all RGNA data have been openly available
 for a 90-day window after the data are collected.
 Access to the proprietary data from times before
 2004 has been granted to the University of Gua-
 dalajara via a negotiated legal agreement. Logisti-
 cal factors limited our access to data collected
 before mid-2001 to one station-day per week
 [Marquez-Azua and DeMets, 2003]. Daily data
 are used for times after mid-2001.

[8] Operation of the RGNA network commenced
 at 14 stations during February to April of 1993 and
 at a 15th station (CAMP) in September of 1995.
 All 15 stations were originally equipped with
 Ashtech LM-XII3 receivers and antennas, which
 acquire coarse-acquisition (C/A) code and L1 and
 L2 phase information but do not collect P-code
 observables under antispoofing conditions. In
 February of 2000, the equipment at station INEG

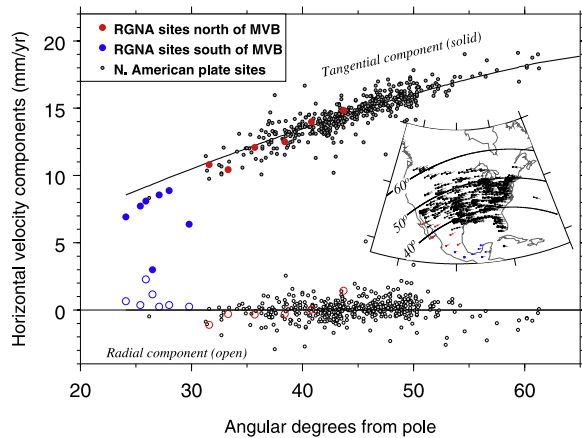


Figure 2. Components of North American plate GPS velocities that are locally parallel (tangential) and orthogonal (radial) to small circles centered on the angular velocity vector that best describes North American plate motion relative to ITRF05. Inset shows the locations of stations used to determine the best-fitting angular velocity vector given in Table 2. The small circles labeled 40°, 50°, and 60° in the inset indicate angular distances from the best-fitting pole and are the same as on the horizontal axis of the upper panel. Blue and red symbols indicate RGNA stations located south and north of the Mexican Volcanic Belt, respectively. Uncertainties are omitted for clarity but are typically $\pm 1 \text{ mm a}^{-1}$ or smaller.

178 was upgraded to a dual-frequency, P-code Trimble
179 receiver and choke ring antenna. Upgrades to
180 dual-frequency, P-code Trimble receivers with
181 Zephyr geodetic antennas occurred at 13 additional
182 stations in January of 2003 and at the remaining
183 station (FMTY) in September of 2003. Readers are
184 referred to MD2003 and www.inegi.org.mx/inegi
185 for additional information about the RGNA
186 network.

187 [9] Physical relocations of the GPS antennas have
188 occurred at least once since 1993 at nine of the
189 15 RGNA stations. Only one of these antenna
190 relocations merits discussion, namely, the reloca-
191 tion in August of 2001 of the antenna at station
192 TOLU to a location 625 m away. Prior to this
193 antenna relocation, the station moved erratically,
194 including 50 mm of subsidence in the 3 years prior
195 to the antenna relocation. No further vertical move-
196 ment has occurred since the antenna was relocated
197 and the horizontal components of the station
198 motion are also well behaved. It thus seems likely
199 that instability of the building or monument that
200 hosted the antenna prior to its relocation was the
201 source of the erratic station behavior, rather than
202 volcanic deformation or localized subsidence due to

groundwater withdrawal, as were postulated by
MD2003. 203 204

[10] Precise geodetic ties between the old and new
RGNA antenna locations are not available for any
of the stations. We therefore estimate all antenna
offsets as part of our postprocessing of the station
coordinate time series. All of the Ashtech antennas
exhibit sudden 25–50 mm westward offsets in
their estimated phase center longitudes in mid-
August of 1999 even though none of the antennas
was physically relocated then [Marquez-Azua and
DeMets, 2003]. These offsets coincided with the
installation of new Ashtech receiver firmware that
was designed to handle the GPS week roll-over
that occurred at that time. Given that other types of
GPS receivers did not exhibit similar shifts in their
antenna phase centers during the GPS week roll-
over in 1999, it seems likely that the Ashtech LM-
XII3 receiver firmware prior to August of 1999
corrupted one or both of the phase or code mea-
surements that were collected prior to this time.
Further evidence for a bias in the eastward com-
ponents of the estimated station motions before
1999 is given below. 205 206 207 208 209 210 211 212 213 214 215 216 217 218 219 220 221 222 223 224 225 226

[11] We also use continuous GPS data from 448 sites
outside of Mexico (Figure 2) to estimate an angular
velocity vector for the North American plate rela-
tive to ITRF05. All 448 stations have operated
continuously for 3 years or longer and are located
outside deforming areas of the western United
States and Canada [Bennett *et al.*, 1999] and
outside areas of significant postglacial rebound in
Canada and the north central and northeastern
United States [Calais *et al.*, 2006; Sella *et al.*,
2007]. 227 228 229 230 231 232 233 234 235 236 237

4. Methods 238

4.1. GPS Station Velocities and Uncertainties 239 240

[12] We processed all of the GPS data described
above with GIPSY software (release 4) from the Jet
Propulsion Laboratory (JPL). We apply a precise
point-positioning analysis strategy [Zumberge *et al.*,
1997] and use fiducial-free satellite orbits and
satellite clock corrections from JPL. Daily station
locations are estimated initially in a no-fiducial
reference frame [Heflin *et al.*, 1992] and are trans-
formed to ITRF2005 [Altamimi *et al.*, 2007] using
daily seven-parameter Helmert transformations
from JPL. Postprocessing procedures are also ap-
plied to estimate and remove spatially correlated
241 242 243 244 245 246 247 248 249 250 251 252

t2.1 **Table 2.** Best-Fitting North American Plate Angular Velocity Vector^a

		Angular Velocity					Covariances					
Plate	N	χ^2_ν	Latitude	Longitude	ω	σ_{xx}	σ_{yy}	σ_{zz}	σ_{xy}	σ_{xz}	σ_{yz}	
NA	448	1.35	-6.80	-84.78	0.189	19.4	419.4	272.0	-3.4	3.7	-310.6	

^aAngular velocity vectors specify plate motion in ITRF2005, with positive angular rotation rates corresponding to counterclockwise rotation about the pole. N is the number of GPS site velocities used to determine the best-fitting angular velocity vector. Here χ^2_ν is the weighted least-squares fit divided by the number of velocity components ($2 \times N$) minus 3, the number of parameters adjusted to fit the data. All covariances are propagated linearly from the GPS site velocity uncertainties and have been rescaled so that the final χ^2_ν equals 1.0. The rotation rate ω has units of degrees per million years. Angular velocity covariances are Cartesian and have units of 10^{-12} radians² per Ma². Abbreviation: NA, North American plate.

253 noise in the daily station locations [Marquez-Azua
254 and DeMets, 2003], resulting in typical daily
255 scatter of 1–3 mm in the horizontal station coordi-
256 nates relative to running 10-day average loca-
257 tions. Linear regression of the three geocentric
258 station coordinates, including corrections for any
259 offsets due to antenna hardware changes or relo-
260 cations, is used to estimate station velocities.

261 [13] An empirically derived error model that approx-
262 imates the white and flicker noise in each station
263 time series and incorporates 1 mm per \sqrt{a} of
264 assumed random monument walk [Mao et al.,
265 1999] is used to estimate the velocity uncertain-
266 ties. Our estimates of the amplitudes of the white
267 and flicker noise are similar to those reported by
268 Williams et al. [2004] for the SOPAC global
269 solution and give rise to station velocity uncer-
270 tainties of ± 0.5 – 0.9 mm a⁻¹ for most of the
271 RGNA stations spanning the 5.6-year-long period
272 from early 2003 to mid-2008 (Table 1). Langbein
273 [2008] uses best geodetic noise models derived
274 from GPS time series for stations in southern
275 California and Nevada to estimate that the uncer-
276 tainties for 5-year-long GPS time series should
277 range from 0.1 to 0.6 mm a⁻¹ for a range of
278 different monumentation types, modestly smaller
279 than but comparable to the uncertainties we esti-
280 mate for the RGNA time series. Our analysis
281 focuses on deformation signals faster than ~ 1 mm
282 a⁻¹ and is thus robust with respect to these small
283 differences in the estimated velocity uncertainties.
284 Uncertainties at the other 448 North American plate
285 stations, whose time series span 3.0 to 15.6 years,
286 range from ± 0.3 to 2 mm a⁻¹.

288 4.2. North American Plate Reference 289 Frame

290 [14] The North American plate constitutes the
291 natural geological reference frame for describing
292 and interpreting the motions of RGNA stations in
293 mainland Mexico. The motion of the plate relative

to ITRF2005 is strongly constrained by the many
294 continuous GPS stations from undeforming areas
295 of the plate interior. We derived a best-fitting
296 angular velocity vector from the velocities of
297 448 North American plate GPS stations (Figure 2),
298 most ($\sim 75\%$) of which are located in the central
299 and eastern United States. The angular velocity
300 vector that best fits these velocities (Table 2) is
301 determined using fitting functions described by
302 Ward [1990]. For reasons described by Argus
303 [1996] and Blewitt [2003], Earth’s center of mass
304 is the appropriate geo-origin for tectonic studies
305 such as this. We thus corrected all of the RGNA
306 and North American plate station velocities for the
307 estimated motion of the ITRF2005 geocenter rela-
308 tive to Earth’s center of mass before inverting those
309 velocities to determine their best-fitting angular
310 velocity vector. On the basis of results reported
311 by Argus [2007], we apply respective corrections
312 of 0.3, 0.0, and 1.2 mm a⁻¹ to the X, Y, and Z
313 Cartesian station velocity components. 314

[15] The residual components of the 448 North Amer-
315 ican plate GPS station velocities (Figure 2) have a
316 weighted root-mean-square misfit of 0.63 mm a⁻¹,
317 close to the lower end of the ± 0.3 to 2 mm a⁻¹ range of
318 the estimated velocity uncertainties. Reduced chi-
319 square for the best-fitting angular velocity vector is
320 1.35, indicating that the average velocity misfit is
321 $\sim 15\%$ (i.e., $\sqrt{1.35}$) larger than its assigned
322 uncertainty. The WRMS misfits are therefore only
323 ~ 0.1 mm a⁻¹ larger than the average estimated
324 uncertainties of ± 0.5 – 0.6 mm a⁻¹. This difference
325 is too small to affect our analysis, which focuses on
326 deformation that is faster than ~ 1 mm a⁻¹. 327

[16] Some of the stations whose velocities are used
328 to estimate North American plate motion lie west of
329 the Rockies and Rio Grande rift (Figure 2), where
330 slow deformation may occur. We thus inverted the
331 velocities of only those stations that lie east of the
332 Rockies and Rio Grande rift in order to examine
333 whether this significantly alters our estimate of
334 North American plate motion in Mexico. The 335

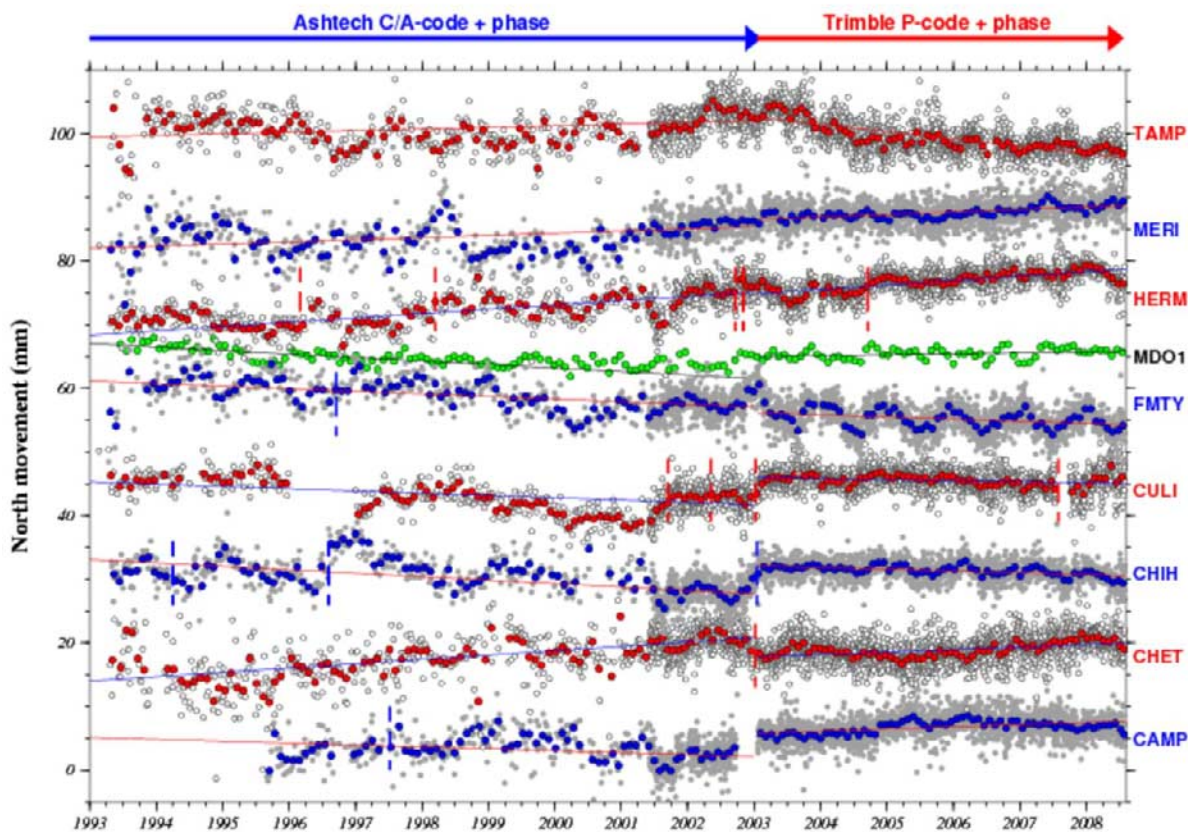


Figure 3. Time series of north components of GPS station coordinates for RGNA stations north of the Mexican Volcanic belt and in the Yucatan peninsula and station MDO1 in southern Texas. Site motions are specified relative to the North American plate (Table 2). Vertical dashed lines show times of offsets that have been estimated and removed from the station time series. Gray and open circles show daily station positions. Monthly average station positions are shown by green, red, and blue circles. Solid lines best fit the station coordinates from 1993.0 to 2001.5, the interval spanned by the codeless Ashtech data, and 2003.0 to 2008.6.

336 alternative best-fitting angular velocity vector predicts station motions in Mexico that differ by no
 337 more than 0.02 mm a^{-1} from the motions that are
 338 predicted by the angular velocity vector given in
 339 Table 2, too small to affect any aspect of the
 340 analysis below.

342 [17] All of the station velocities and coordinate
 343 time series described below were transformed to
 344 a North American plate frame of reference by
 345 subtracting the plate motion predicted at each site
 346 by the best-fitting angular velocity vector (Table 2).
 347 Uncertainties in the best-fitting angular velocity
 348 vector were propagated rigorously into all station
 349 velocity uncertainties quoted in the text and shown
 350 in the figures.

352 5. Results

353 [18] Our results are presented in two stages. We
 354 first use the station coordinate time series for nine

RGNA sites with linear motion (Figures 3–5) to
 test for significant differences in the station velocities
 before and after the GPS receiver changeover that
 occurred in 2003. We then use the new RGNA site
 velocities to evaluate the fits of two geologically
 plausible models for the present motion and
 deformation of Mexico. The analysis concludes
 with descriptions of the motions of stations OAXA
 and TOLU (Figure 5), which exhibit the elastic
 effects of steady interseismic locking and transient
 slip along the Cocos plate subduction interface, and
 of stations COLI and INEG, whose motions are
 strongly influenced by the coseismic and postseismic
 effects of subduction thrust earthquakes off the
 coast of western Mexico on 9 October 1995 and
 22 January 2003 (Figure 8).

5.1. RGNA Stations With Linear Motions

[19] Figures 3–5 show the coordinate time series
 for all nine RGNA stations with linear motions

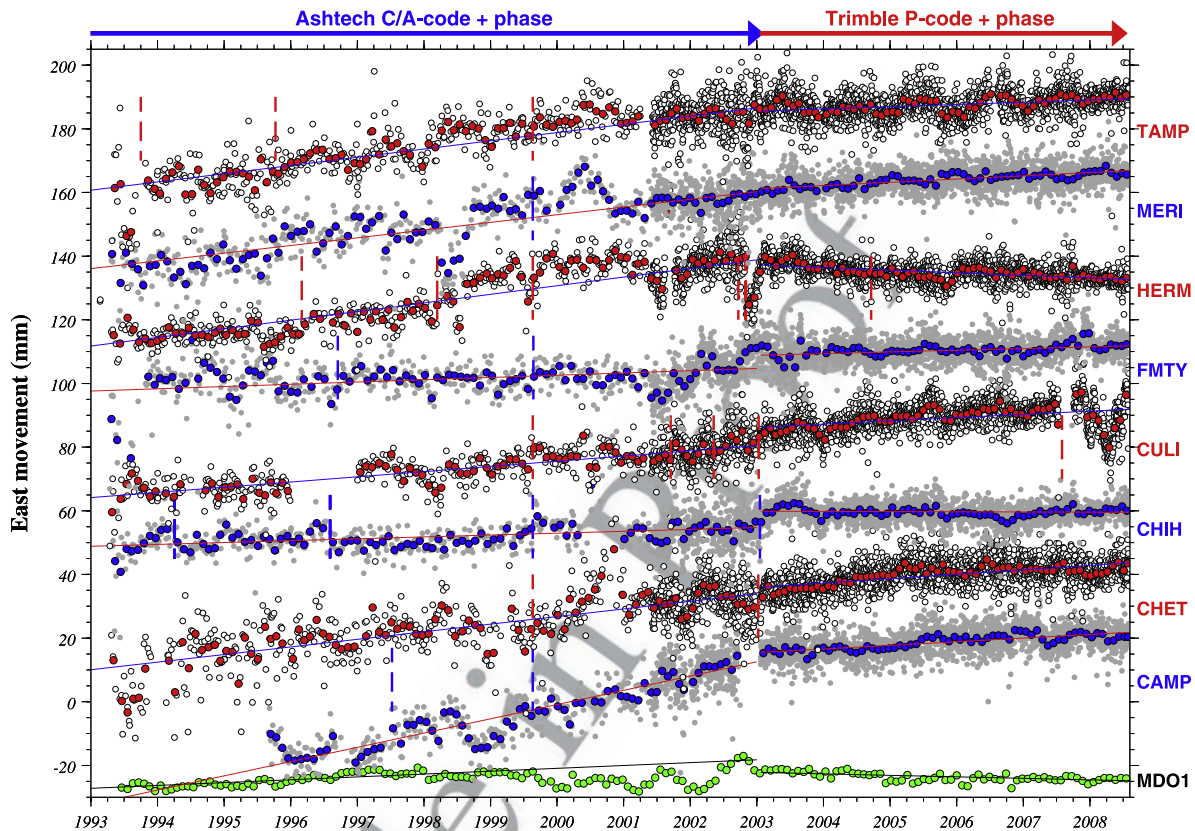


Figure 4. Time series of east component of GPS station coordinates for RGNA stations north of the Mexican Volcanic belt and in the Yucatan peninsula, and station MDO1 in southern Texas. See caption to Figure 3 for additional information.

374 from mainland Mexico and one station (MDO1) in
 375 southern Texas at which continuous P-code carrier
 376 phase GPS measurements have been made since
 377 1993. The steady motions at the RGNA sites
 378 provide a strong basis for comparing the site
 379 motions during the period from 1993 to 2003,
 380 when data at all nine stations were collected by
 381 Ashtech C/A-code receivers, to the motions since
 382 2003.0, during which P-code Trimble receivers
 383 have operated at all nine sites.

384 [20] We first test for significant changes in the
 385 north components of the station motions before
 386 and after 2003 by deriving separate best-fitting
 387 lines for the daily station coordinates from 1993
 388 to 2003 and for 2003 to the present (mid-2008).
 389 The slopes that best fit the RGNA station latitudes
 390 during these two time periods differ on average by
 391 0.7 mm a^{-1} , with differences at the individual sites
 392 of 0.2 mm a^{-1} to 1.3 mm a^{-1} (Figure 3). None of
 393 the changes in slope at the nine RGNA stations are
 394 significant at the 95% confidence level.

395 [21] At site MD01 in Texas, where dual-frequency
 396 P-code GPS data has been collected continuously

since 1993, the slopes that best fit the daily station
 coordinates for times before and after 2003 differ
 by 0.8 mm a^{-1} . The difference in slope at MDO1
 before and after 2003 is thus comparable to that
 for the RGNA sites, where the differences average
 0.7 mm a^{-1} .

[22] We conclude that the north (latitudinal) com-
 ponents of the RGNA station motions are well
 determined for the entire period that the sites have
 operated. Transient deformation episodes that were
 recorded before 2003 at RGNA sites OAXA and
 TOLU (described below) were dominated by
 north–south station movements and by implication
 were also reliably recorded.

[23] The east components of motion at the nine
 RGNA stations are less consistent (Figure 4). The
 differences between the best-fitting rates for the
 two time periods range from 0.2 to 3.4 mm a^{-1} and
 average 1.6 mm a^{-1} , more than twice the average
 slope difference for the station latitudes. At seven
 of the nine RGNA sites, the eastward site motion
 before 2003.0 was faster by $1\text{--}3.5 \text{ mm a}^{-1}$ than

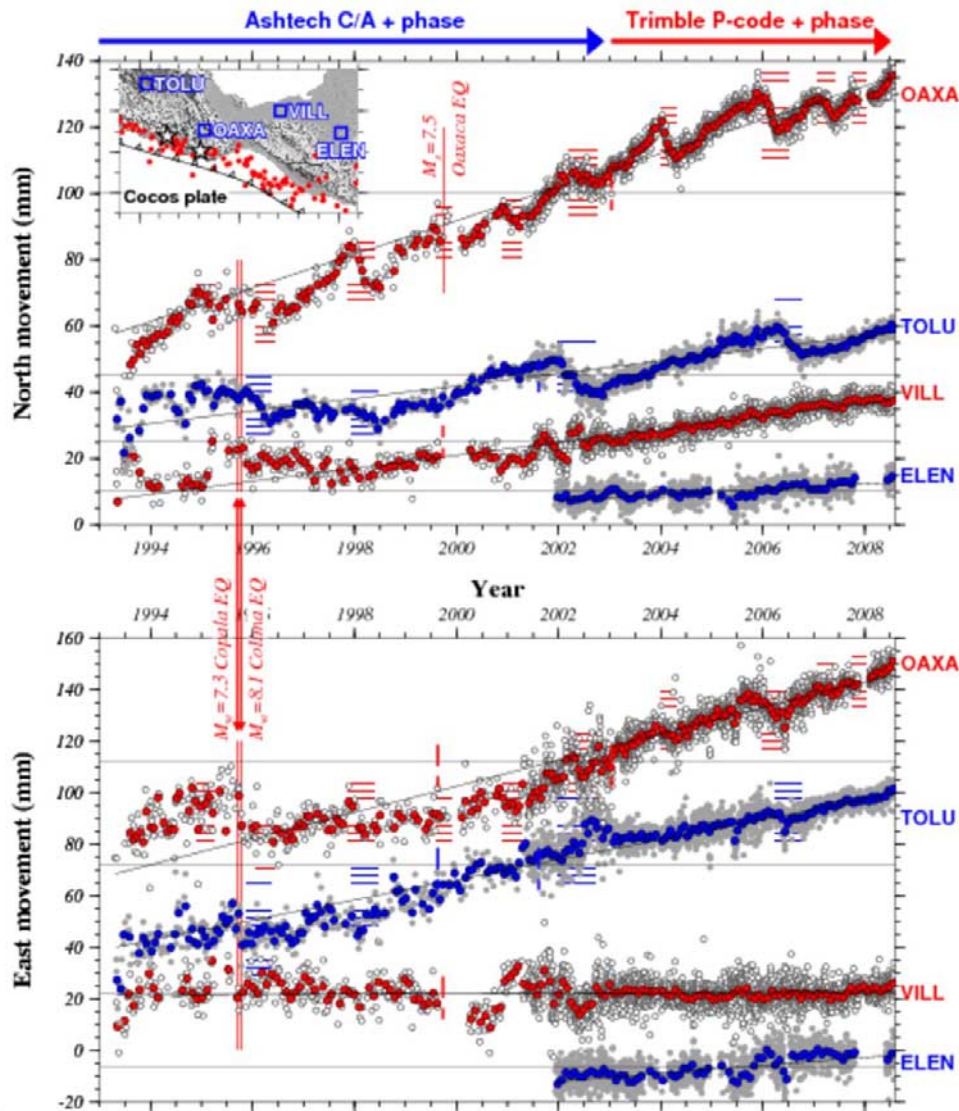


Figure 5. (top) North and (bottom) east components of GPS station coordinates from 1993 to 2008 for RGNA stations in southern Mexico and station ELEN in Guatemala. Patterned areas specify periods of southward station motion that coincide with transient slip along the subduction interface. See caption to Figure 3 for additional information. Inset shows topography, GPS station locations, and epicenters (red circles) of 1963–2008 earthquakes with magnitudes greater than 5.5 and depths above 40 km from the U.S. Geological Survey National Earthquake Information Center files. Black stars in inset show locations of the $M_w = 7.3$ 14 September 1995 Copala and $M_s = 7.5$ 30 September 1999 Oaxaca earthquakes.

419 after 2003.0 (Figure 4), and at five sites, the change
420 in slope is statistically significant.

421 [24] The evidence thus indicates that there was a
422 systematic, significant change in the apparent east
423 component of the station motions in early 2003,
424 coinciding with the change in GPS equipment at
425 most of the stations. All four stations in and near
426 the Yucatan peninsula that were reported by
427 MD2003 as having anomalously rapid eastward
428 motion slowed down significantly after 2003 (com-

pare blue and red velocities at sites CAMP, CHET,
429 MERI, and VILL in Figure 6). 430

[25] We thus conclude that east components of the
431 RGNA station motions for times when the Ashtech
432 LM-XII3 codeless receivers were operating, pri-
433 marily before 2003.0, are unreliable. We suspect
434 but cannot show that the receiver firmware or
435 hardware corrupted the raw data. The coordinate
436 time series for station MDO1 (Figures 4 and 5) and
437 other P-code stations in the southern United States
438

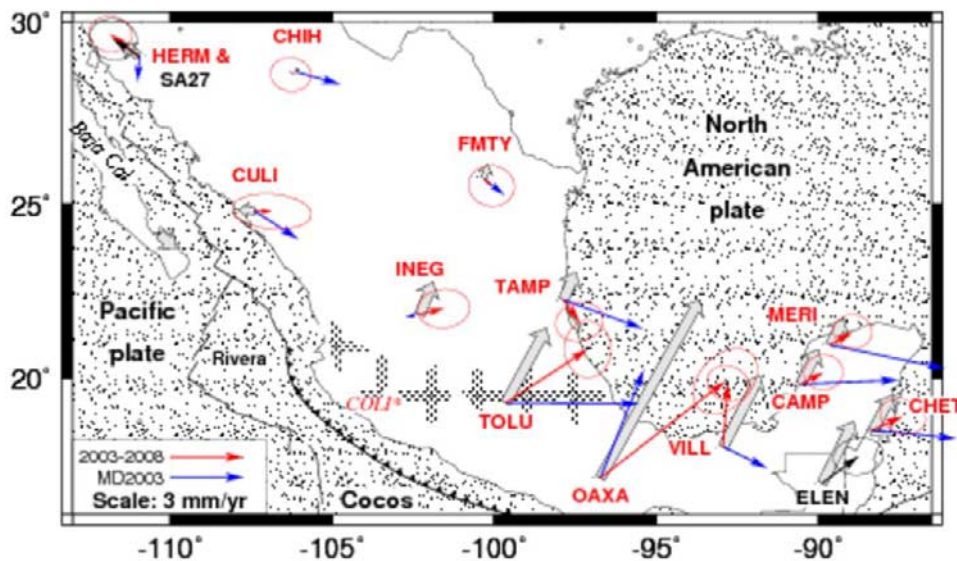


Figure 6. RGNA station velocities relative to the North American plate for sites on mainland Mexico. Red arrows show velocities determined solely from 2003 to 2008.6 P-code carrier phase GPS data and blue arrows show velocities determined by *Marquez-Azua and DeMets* [2003] from Ashtech codeless data from 1993 to 2001.5. Gray arrows indicate velocities predicted by an elastic half-space model with a fully coupled Mexican subduction interface and faults in the Gulf of California, as described in the text. The velocity for station COLI is severely impacted by postseismic effects of the $M_w = 8.0$ 9 October 1995 earthquake and $M_w = 7.5$ 22 January 2003 earthquake and is not depicted. Uncertainty ellipses are 2-D, 1- σ .

439 that have operated since at least the mid-1990s
440 (not shown) do not exhibit significant changes
441 in their north or east components of motion
442 before and after 2003, further reinforcing the above
443 conclusion.

445 5.2. Velocity Field Analysis

446 [26] We next undertake statistical comparisons of
447 three realizations of the RGNA station motions to
448 velocity fields that are predicted by two models for
449 the present motion and deformation of Mexico. In
450 the first model, we assume that all of mainland
451 Mexico moves with an undefining North Amer-
452 ican plate. In the second model, we assume that the
453 elastic effects of frictional coupling across the
454 Mexican subduction zone and strike-slip faults in
455 the Gulf of California are superimposed on the
456 plate motion. Further details about both models are
457 given below.

458 [27] The three RGNA velocity fields used for this
459 comparison consist of the MD2003 velocities for
460 1993 to 2001.5, velocities from 1993 to 2003.0,
461 which span the entire period of Ashtech LM-XII3
462 codeless measurements, and velocities from 2003.0
463 to August of 2008 (Table 1), which span the period
464 of Trimble P-code, carrier phase measurements at
465 the RGNA sites. Each velocity field includes 12 of

the 13 RGNA stations, consisting of all nine line- 466
467 arly moving sites (Figures 3 and 4) and the veloc-
468 ities for INEG, OAXA, and TOLU, whose long-
469 term motions are contaminated to varying degrees
470 by transient deformation related to the Mexican
471 subduction zone (described in section 5.3). We
472 excluded site COLI from this part of the analysis
473 because its motion is too severely disrupted by the
474 coseismic and postseismic effects of the 9 October
475 1995 $M_w = 8.0$ and 22 January 2003 earthquakes
476 (described in section 5.3.2) to recover any useful
477 information about either the long-term motion or
478 interseismic elastic shortening at this site.

[28] We use weighted root-mean-square (WRMS) 479
480 misfits to evaluate the fits of both models to the
481 three velocity fields described above. We gauge
482 the acceptability of the fit of each model to the
483 observed velocities by comparing it to the
484 0.63 mm a^{-1} WRMS misfit of the angular veloc-
485 ity that best fits the 448 North American plate
486 station velocities. The WRMS misfit for these
487 448 stations should approximate the underlying
488 velocity dispersion for GPS stations located in a
489 plate interior and therefore should be an approxi-
490 mate limit on how well we might expect any model
491 to fit the RGNA station velocities. Although more
492 complex physical models for the present motion
493 and deformation of Mexico could be postulated

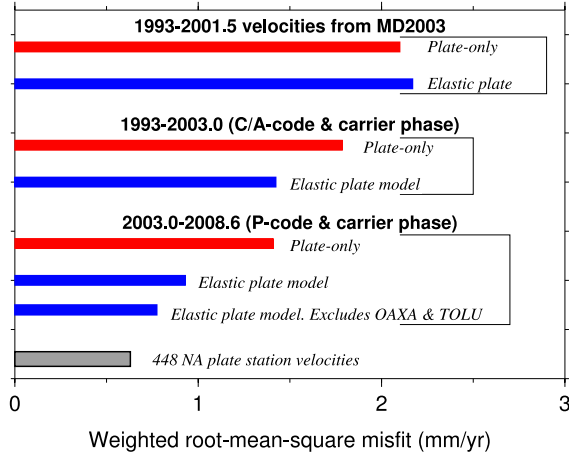


Figure 7. Weighted root-mean-square misfits of the North American plate angular velocity vector (plate-only) and elastically modified plate models to RGNA velocity fields for stations on mainland Mexico. Red and blue bars indicate fits of plate-only and elastic plate models, respectively. The gray bar shows the RMS misfit to the 448 station velocities used to determine the North American plate angular velocity vector. Fits for three realizations of the RGNA velocities are shown: the 1993–2001.5 velocities from *Marquez-Azua and DeMets* [2003], velocities determined from 1993–2003 Ashtech data described in the text, and velocities determined from 2003.0–2008.6 P-code and carrier phase GPS data. Unless otherwise noted, the fits are determined for 12 of the 13 RGNA stations on the mainland and exclude only station COLI due to postseismic effects from the 9 October 1995 and 22 January 2003 earthquakes.

494 and tested, we demonstrate below that the RGNA
495 station velocities are fit at the level of their uncer-
496 tainties by one of the two simple models that we
497 tested.

498 5.2.1. Plate-Only Model

499 [29] The simplest of the two models we examined
500 assumes that the motion of mainland Mexico is
501 well described by the angular velocity vector that
502 best fits the 448 North American station velocities
503 (Table 2). The residual motions of the RGNA
504 stations relative to the North American plate for
505 the 1993–2001.5 MD2003 site velocities (blue
506 arrows in Figure 6) clearly reveal the east-directed
507 velocity bias described by MD2003. In contrast,
508 the residual motions for the new 2003–2008.6
509 velocities show no obvious systematic bias (red
510 arrows in Figure 6). The WRMS misfit to the 1993–
511 2001.5 MD2003 station velocities is 2.1 mm a^{-1}
512 (Figure 7), more than three times larger than for
513 the 448 North American plate station velocities.

We measured the statistical significance of the
514 difference between these two fits using a F ratio
515 test comparison of the ratio of the values of
516 reduced chi-squared for the two models. The fits
517 differ at a high confidence level ($p = 8 \times 10^{-7}$).
518 The MD2003 RGNA station velocities therefore
519 differ significantly from the velocities predicted by
520 the North American plate angular velocity vector.
521

[30] The WRMS misfit of the plate-only model to
522 the station velocities averaged from 1993 through
523 early 2003 is 1.8 mm a^{-1} (Figure 7), only margin-
524 ally better than for the 1993–2001.5 MD2003
525 velocity field (Figure 7). This misfit also differs
526 at high confidence level from the misfit to the 448
527 North American plate station velocities.
528

[31] The WRMS misfit of the plate-only model to
529 the 2003.0–2008.6 RGNA velocities is 1.4 mm a^{-1}
530 (Figure 7), smaller than for the other two velocity
531 fields. The velocities of all of the stations north of
532 the volcanic belt except HERM are well fit by the
533 plate-only model (red arrows in Figure 6). The
534 motions at sites in central Mexico, southern Mex-
535 ico, and the Yucatan peninsula however differ
536 systematically from the plate-only model predic-
537 tions. The WRMS misfit is still more than twice the
538 magnitude of the WRMS misfit for the 448 North
539 American plate station velocities and differs at high
540 confidence level ($p = 1 \times 10^{-7}$). We conclude that
541 none of the RGNA velocity fields are well fit by a
542 plate-only model.
543

544 5.2.2. Velocity Field Analysis: Elastically 545 Modified Plate Model

[32] The second model we tested superimposes the
546 interseismic elastic effects of frictional coupling
547 across faults in the Gulf of California and the
548 Mexican subduction zone on North American plate
549 motion. The elastic response at each RGNA station
550 due to assumed locking of both sets of faults is
551 determined using homogeneous elastic half-space
552 modeling. Each of the strike-slip fault segments in
553 the Gulf of California is assumed to be locked from
554 the surface to a maximum depth of 10 km, repre-
555 senting an approximate conservative depth limit for
556 the seismogenic zone in the Gulf of California
557 [Goff *et al.*, 1987]. The interseismic elastic re-
558 sponse is determined assuming that a 48 mm a^{-1}
559 slip deficit accumulates along each strike-slip fault
560 in the gulf, consistent with the average slip rate in
561 the Gulf over the past 0.78 Ma [DeMets, 1995].
562

[33] The Mexican subduction zone is approximated
563 with 360 nodes whose locations in the elastic half
564



565 space mimic the geography of the subduction zone
566 (node locations are shown in Figure 1) and define a
567 planar fault that dips 15° beneath the continent and
568 extends downdip to a depth of 25 km, the approx-
569 imate lower limit of seismogenic slip for the Mex-
570 ican subduction interface [Suarez and Sanchez,
571 1996; Hutton *et al.*, 2001; Yoshioka *et al.*, 2004;
572 Correa-Mora *et al.*, 2008]. The elastic responses at
573 the RGNA sites are determined by imposing trench-
574 normal back slip at each node that is equal in
575 magnitude to the convergence rate calculated
576 from either the Rivera-North America [DeMets
577 and Wilson, 1997], Cocos-North America [DeMets,
578 2001], or Cocos-Caribbean [DeMets, 2001] angular
579 velocity vector, depending on the node location.
580 The model thus implicitly assumes that the subduc-
581 tion interface is fully and homogeneously coupled
582 by friction at depths above 25 km. Although this
583 model clearly oversimplifies the interseismic be-
584 havior and geometry of the Mexican subduction
585 interface, the RGNA stations are too widely spaced
586 and in most cases too far from the trench to merit
587 any additional model complexity. As described
588 below, this surprisingly simple model approximates
589 the northeast-directed elastic shortening of main-
590 land Mexico well enough to fit most of the RGNA
591 station velocities to better than 1 mm a^{-1} .

592 [34] The predicted elastic responses at the RGNA
593 stations (shown by the gray arrows in Figure 6)
594 range from less than 0.1 mm a^{-1} at sites in
595 northern Mexico to 8.4 mm a^{-1} at station OAXA
596 in southern Mexico. Changes of $\pm 5^\circ$ in the as-
597 sumed 15° dip of the subduction interface alter the
598 rates that are predicted by our elastic half-space
599 model by $\sim 20\%$, representing one source of un-
600 certainty in our elastic model predictions.

601 [35] The WRMS misfit of the elastically modified
602 model to the MD2003 velocity field is nearly the
603 same as for the plate-only model (Figure 7) and
604 still differs at high confidence level ($p = 9 \times 10^{-7}$)
605 from the WRMS misfit to the 448 North American
606 station velocities. Similarly, the WRMS misfit to
607 the 1993–2003 station velocities (1.4 mm a^{-1}) also
608 differs from that for the 448 North America station
609 velocities at high confidence level ($p = 4 \times 10^{-5}$).
610 Neither of the two RGNA velocity fields that are
611 determined from the Ashtech data are consistent
612 within acceptable limits with the predictions of the
613 plate-only or elastically modified models.

614 [36] The WRMS misfit of the elastically modified
615 model to the 2003–2008.6 P-code velocity field is
616 0.93 mm a^{-1} 35% smaller than the WRMS misfit
617 of the plate-only model (Figure 7). More than half

of the variance (56%) between the measured and
predicted station velocities is contributed by the
poor fits at stations OAXA and TOLU (Figure 6).
The poor fits are not surprising given that the
motions of both stations are influenced by transient
slip events (Figure 8), which are ignored in our
simplified elastic model. In addition, the approx-
imations that we use to construct our elastic model
influence the motions predicted by that model at
OAXA and TOLU by as much as $1\text{--}3 \text{ mm a}^{-1}$.
The misfits thus could be reduced if we changed
one or more of our modeling assumptions.

[37] If we exclude the velocities at OAXA and
TOLU, the WRMS misfit of the elastically modified
model to the remaining 10 RGNA station velocities
is only 0.77 mm a^{-1} , close to the 0.63 mm a^{-1}
WRMS misfit for the 448 North American plate
stations. The values of reduced chi-square associ-
ated with these two fits do not differ significantly
($p = 0.42$). The velocities of the stations far from
the subduction zone are thus consistent with the
hypothesis that mainland Mexico moves with the
North American plate after the elastic effects of
locked plate boundary faults are accounted for.

[38] Although the poor fits to the velocities at sites
OAXA and TOLU prevent us from concluding that
areas south of the Mexican volcanic belt also move
with the North American plate, Correa-Mora *et al.*
[2008] find that the directions of 30 GPS stations in
Oaxaca, south of the volcanic belt, differ by less
than 1° from the Cocos-North America plate con-
vergence direction after correcting the station time
series for the influence of transient slip episodes.
Their results thus indicate that southern Mexico
moves with the North America plate, in accord
with structural evidence for insignificant Quater-
nary displacement across faults in the Mexican
volcanic belt [Ferrari and Rosas-Elguera, 2000;
Suter *et al.*, 2001; Langridge *et al.*, 2000].

5.3. RGNA Stations With Nonlinear Motions

[39] All four of the RGNA stations that are located
within several hundred kilometers of the Mexican
subduction zone exhibit nonlinear motions (Figures 5
and 8) that represent superpositions of subduc-
tion-related processes and North American plate motion.
Their coordinate time series provide useful new
information about the timing, style, and spatial
extent of deformation in southern Mexico and are
described below. Modeling of these and other non-
RGNA time series is underway to relate all four time

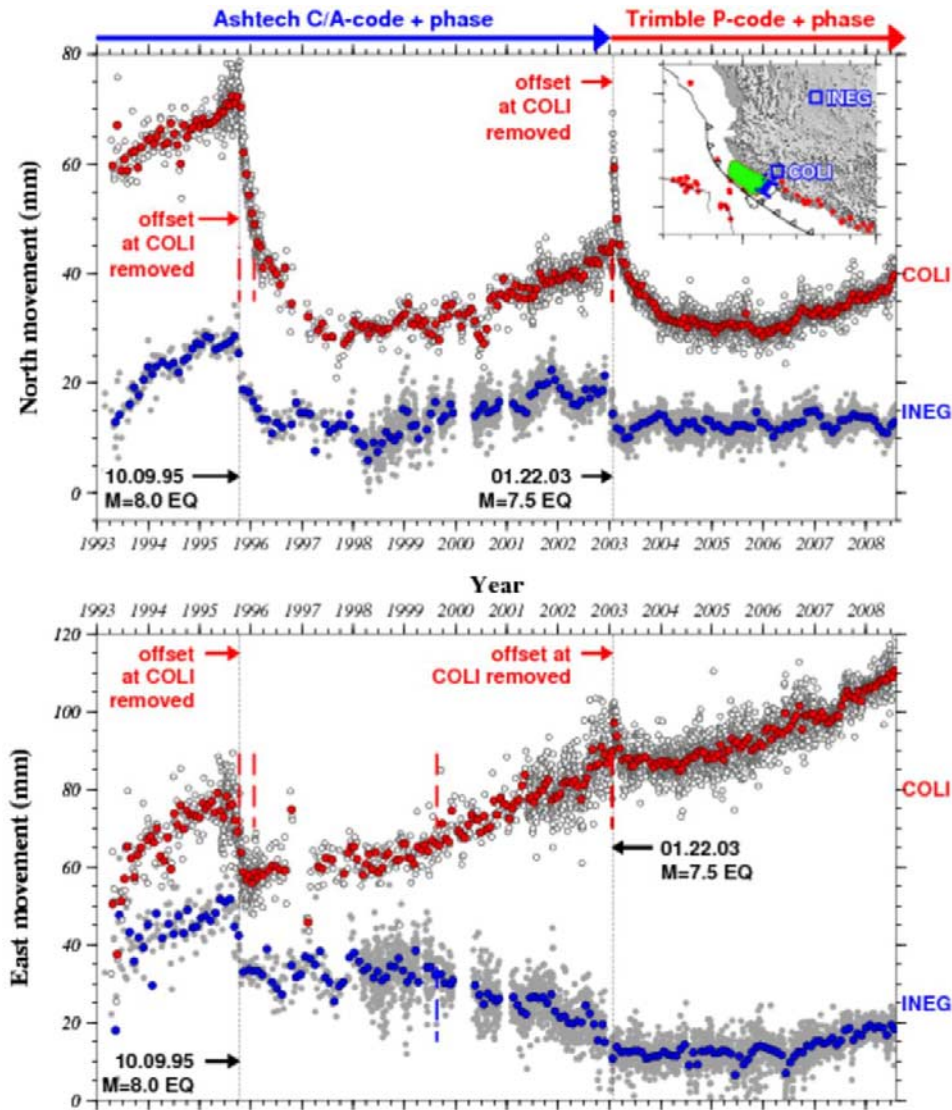


Figure 8. Modified (top) north and (bottom) east components of GPS station coordinates from 1993 to 2008 for RGNA stations COLI and INEG in western Mexico. Arbitrary offsets at COLI for the 9 October 1995, $M_w = 8.0$ Colima-Jalisco and 22 January 2003, $M_w = 7.5$ Tecoman earthquakes have been removed from the time series in order to enhance the postseismic and interseismic phases of the time series. Inset shows topography, GPS station locations, and epicenters (red circles) of 1963–2008 earthquakes with magnitudes greater than 5.5 and depths above 40 km from the U.S. Geological Survey National Earthquake Information Center files. See caption for Figure 3 for additional information about the symbols and dashed lines. Green and blue shaded regions in inset show extent of the 1995 and 2003 earthquakes. See caption to Figure 3 for additional information.

670 series to earthquake cycle effects associated with the
671 Cocos and Rivera plate subduction interfaces.

672 5.3.1. Effects of Transient Slip Events in 673 Southern Mexico

674 [40] Stations OAXA and TOLU lie onshore from
675 the Oaxaca and Guerrero segments of the Mexican
676 subduction zone (Figure 5), where continuous
677 measurements at these and other GPS stations
678 reveal evidence for occasional transient slip events

along parts of the subduction interface downdip 679
from the seismically active areas of the subduction 680
interface [Lowry *et al.*, 2001; Kostoglodov *et al.*, 681
2003; Franco *et al.*, 2005; Brudzinski *et al.*, 2007; 682
Larson *et al.*, 2007; Correa-Mora *et al.*, submitted 683
manuscript, 2009]. Although the net motions of 684
both stations since 1993 have been northeast with 685
respect to the plate interior, both stations have 686
alternated between periods of northeast-directed 687
motion that last from one to several years and 688



689 periods of opposite-sense, trenchward motion that
690 last from 2 to 6 months.

691 [41] Ten periods of transient slip were recorded at
692 OAXA between 1993 and mid-2008 (Figure 5), all
693 dominated by south-directed motion, but including
694 lesser west-directed motion. The magnitudes of the
695 SSW-directed transient offsets range from 5 mm to
696 15 mm, of which the largest were in early 1998,
697 early 2004, and early 2006, and smaller episodes
698 were in early 1995, early 1996, late 1999, late
699 2000, mid-2002, and early 2007. Modeling of the
700 transient slip events in 2004, 2006, and 2007
701 indicates that all three occurred beneath eastern
702 Oaxaca downdip from the seismogenic zone
703 [Brudzinski *et al.*, 2007; Correa-Mora *et al.*,
704 2008; Correa-Mora *et al.*, submitted manuscript,
705 2009]. Modeling of the earlier transient slip events
706 has not been undertaken due to the sparse contin-
707 uous GPS station coverage prior to 2004.

708 [42] Two moderate- to large-magnitude earth-
709 quakes occurred along the Guerrero and Oaxaca
710 segments of the Mexican subduction zone between
711 1993 and mid-2008: the 14 September 1995 $M_w =$
712 7.3 Copala earthquake, a thrust-faulting event
713 along the Guerrero trench segment ~ 200 km west
714 of OAXA (see Figure 5 inset), and the 30 Septem-
715 ber 1999 $M_s = 7.5$ Oaxaca earthquake, a normal
716 faulting event within the subducting Cocos plate
717 beneath central Oaxaca. During the Copala earth-
718 quake, an offset of ~ 10 mm toward the rupture
719 zone west of Oaxaca was recorded at station
720 OAXA (shown in Figure 5, bottom). During the
721 1999 Oaxaca intraslab earthquake, no coseismic
722 offset was recorded at OAXA. Interestingly, the
723 1999 earthquake occurred during the transient slip
724 event recorded at OAXA in late 1999, suggesting
725 the possibility that one may have triggered the
726 other. The OAXA station positions for this period
727 are, however, too noisy to determine whether the
728 earthquake preceded the initiation of transient slip
729 or vice versa.

730 [43] Fewer transient slip events have been recorded
731 at station TOLU, which is located in the Mexican
732 volcanic belt inland from the Guerrero segment of
733 the subduction zone (Figure 5). Three or possibly
734 four transient slip events have been recorded since
735 1993, each dominated by 7–15 mm of southward
736 motion toward the Guerrero segment of the Mex-
737 ican subduction zone. The earliest transient slip
738 episode began in late 1995 and is clearly shown by
739 the reliably recorded N–S component of motion at
740 TOLU. From campaign GPS measurements in
741 1995, 1996, and 1998 along the coast of Guerrero,

Larson et al. [2004] hypothesize that transient slip 742
occurred beneath Guerrero in late 1995. The 743
RGNA measurements confirm this. 744

[44] Transient slip events that were recorded at 745
TOLU in early 1998, 2001–2002, and 2006 746
(Figure 5) coincide with transient slip events 747
beneath Guerrero that are described and modeled 748
by *Lowry et al.* [2001], *Kostoglodov et al.* [2003], 749
and *Larson et al.* [2007]. Readers are referred to 750
those studies for additional information. 751

5.3.2. COLI and INEG: Effects of the 1995 752 and 2003 Western Mexico Earthquakes 753

[45] The 9 October 1995 $M_w = 8.0$ Colima-Jalisco 754
earthquake and 22 January 2003 $M_w = 7.5$ Tecoman 755
earthquake (Figure 8) ruptured the Rivera/Cocos 756
plate subduction interfaces off the coast of western 757
Mexico. Both caused measurable coseismic and 758
postseismic movements at stations COLI and INEG 759
(Figure 8), which are located 80 km and 400 km 760
inland from the coast, respectively. During the 1995 761
earthquake, COLI was offset by 132 ± 5 mm toward 762
 $S66^\circ W$ [Marquez-Azua *et al.*, 2002], toward the 763
seismologically and geodetically constrained region 764
of maximum coseismic slip [Melbourne *et al.*, 765
1997; Mendoza and Hartzell, 1999; Hutton *et al.*, 766
2001]. Additional trenchward motion occurred dur- 767
ing the following 18 months (Figure 8), consisting 768
largely of ~ 50 mm of southward movement at rates 769
that decayed with time. By early 1998, slow north- 770
eastward movement had resumed, similar to the site 771
motion before the earthquake. 772

[46] Finite element modeling of the COLI coordi- 773
nate time series for 1993 to mid-2001 suggests that 774
three distinct processes contributed to the station 775
motion during this period: (1) steady, northeast- 776
directed elastic shortening due to frictional locking 777
of shallow seismogenic parts of the subduction 778
interface, (2) decaying postseismic fault afterslip 779
in response to time-dependent changes in the 780
coefficient of friction after the 1995 earthquake, 781
(3) decaying viscoelastic relaxation of the elevated 782
stresses in the lower crust and upper mantle after 783
the earthquake [Marquez-Azua *et al.*, 2002]. 784

[47] During the 2003 earthquake, COLI was offset 785
 127 ± 5 mm toward $S34^\circ W$, consistent with the 786
coseismic offsets that were measured at other 787
stations in this region [Schmitt *et al.*, 2007]. The 788
station continued moving to the SSW at increas- 789
ingly slower rates for 18–24 months after the 790
earthquake (Figure 8) and resumed moving slowly 791
to the northeast by early 2006. The similarity of the 792



793 postseismic movements after the 1995 and 2003
794 earthquakes suggests that fault afterslip, viscoelas-
795 tic rebound, and frictional relocking of shallow
796 seismogenic areas of the subduction interface con-
797 trolled the surface deformation at COLI in both
798 cases, providing a solid basis for better understand-
799 ing the physical processes that dictate short-term
800 deformation in this region.

801 [48] Although groundwater withdrawal caused sta-
802 tion INEG to subside more than 1.4 m between
803 early 1993 and August of 2008 (not shown), the
804 rapid station subsidence does not appear to have
805 corrupted its horizontal motion, which mimics
806 many features of the COLI time series since 1993
807 (Figure 8). We attribute the differences in the
808 motions of INEG and COLI to their different
809 distances from the subduction zone, which gives
810 rise to less interseismic elastic shortening at INEG
811 than at COLI, as well as relatively less viscoelastic
812 rebound at INEG after the 1995 and 2003 earth-
813 quakes. We are presently modeling these and other
814 data from the region to better understand the
815 relative contributions of viscoelastic rebound, fault
816 afterslip, and interseismic locking to earthquake
817 cycle deformation in this region.

819 6. Discussion and Conclusions

820 [49] The elastically modified plate model described
821 above is remarkably effective at predicting the
822 newly estimated RGNA velocity field (Figure 6).
823 In particular, our updated velocities for the four
824 RGNA stations in and near the Yucatan peninsula
825 (CAMP, CHET, MERI, and VILL) agree within
826 their uncertainties with the northeast-directed sta-
827 tion motions that are predicted by our simple
828 elastic model (Figure 6). The puzzling eastward
829 bias reported by MD2003 in the velocities for these
830 four stations was thus an artifact of the non-P-code
831 Ashtech data that were used to estimate the
832 MD2003 velocities. Similar eastward biases in
833 the velocities estimated by MD2003 at other
834 RGNA stations (Figure 6) were thus also artifacts
835 of the Ashtech data and are largely gone from the
836 updated velocity field. Overall, the WRMS differ-
837 ence between the model predictions and updated
838 station velocities is only 0.8 mm a^{-1} , comparable
839 to the misfit for the 448 station velocities that were
840 inverted to determine the North American plate
841 angular velocity vector.

842 [50] At station HERM east of the Gulf of California
843 (Figure 6), our elastic model predicts motion of
844 0.8 mm a^{-1} toward $\text{N}55^\circ\text{W}$, the same within uncer-

tainties as the measured velocity of $1.4 \pm 0.6 \text{ mm}$
845 a^{-1} toward $\text{N}53^\circ\text{W} \pm 21^\circ$. Further supporting this
846 result, GPS site SA27, which has operated contin-
847 uously since mid-2003 at a location only 1.5 km
848 from HERM, also moves $1.2 \pm 0.6 \text{ mm a}^{-1}$ toward
849 $\text{N}55^\circ\text{W} \pm 29^\circ$ (Figure 6), nearly the same as HERM
850 and in even better agreement with the elastically
851 predicted motion. Incorporating the elastic effects
852 of locked strike-slip faults in the Gulf of California
853 is thus necessary for fitting these station velocities.
854

[51] Our simple elastic model successfully predicts
855 the northeastward motions of RGNA stations
856 INEG, OAXA, and TOLU in central and southern
857 Mexico (Figure 6) but fits those velocities more
858 poorly than is the case at the other RGNA sites. The
859 poorer fits are due in part to the effects of transient
860 slip episodes at both sites, which influence their
861 estimated motions. Oversimplifications in our elas-
862 tic half-space model also surely contribute to the
863 misfits. We did not attempt to improve the fits by
864 adjusting any of our elastic modeling assumptions
865 or parameters, mainly because the RGNA stations
866 are too widely spaced and too far from the trench to
867 merit such an exercise. We instead refer readers
868 who seek more information about the spatial and
869 temporal characteristics of strain accumulation and
870 release along the Cocos plate subduction interface
871 to detailed modeling studies of GPS measurements
872 at numerous near-coastal stations in Guerrero and
873 Oaxaca [e.g., *Yoshioka et al.*, 2004; *Franco et al.*,
874 2005; *Correa-Mora et al.*, 2008].
875

[52] Although our new velocity field agrees much
876 better with the predictions of our simple elastic
877 model than does the MD2003 velocity field, small
878 differences between the newly measured velocities
879 and the predicted velocities still remain. In partic-
880 ular, the velocities of six of the seven RGNA
881 stations in the volcanic belt, southern Mexico,
882 and the Yucatan peninsula are rotated clockwise
883 from the predicted motions by varying amounts
884 (Figure 6), as is the velocity of station ELEN in
885 northern Guatemala. Random errors in the estimated
886 station velocities are unlikely to cause this system-
887 atic difference. Although the velocity bias is con-
888 sistent with slow eastward motion ($\sim 1 \text{ mm a}^{-1}$ or
889 less) of southern Mexico and northern Guatemala
890 relative to the North American plate, a more
891 conservative interpretation is that the time series
892 for all of these stations are still too short (5 to
893 6 years) to effectively average out any time-
894 correlated variations in the station coordinates that
895 remain coherent over periods of several years or
896 longer. Additional years of observations will help
897



898 to reduce the effect of time-correlated noise. To
899 determine whether GPS system noise might be
900 responsible for some or all of the small remaining
901 eastward velocity bias, we also plan to reprocess
902 the RGNA data using the next generation of
903 satellite orbits and geodetic reference frame prod-
904 ucts that should soon be available from the
905 International GNSS Service.

906 Acknowledgments

907 [53] We thank INEGI for generously providing daily data
908 from the RGNA network, without which this work would not
909 be possible. We thank Luca Ferrari and an anonymous
910 reviewer for their helpful suggestions. This research was
911 funded by National Science Foundation grant EAR-0510553
912 and by the University of Guadalajara, which contributed funds
913 for research exchange visits.

915 References

- 916 Altamimi, Z., X. Collilieux, J. Legrand, B. Garayt, and
917 C. Boucher (2007), ITRF2005: A new release of the Inter-
918 national Terrestrial Reference based on time series of station
919 positions and Earth Orientation parameters, *J. Geophys. Res.*,
920 *112*, B09401, doi:10.1029/2007JB004949.
- 921 Argus, D. F. (1996), Postglacial uplift and subsidence of
922 Earth's surface using VLBI geodesy: On establishing vertical
923 reference, *Geophys. Res. Lett.*, *23*, 973–976.
- 924 Argus, D. F. (2007), Defining the translational velocity of the
925 reference frame of Earth, *Geophys. J. Int.*, *169*, 830–838,
926 doi:10.1111/j.1365-246X.2007.03344.x.
- 927 Bennett, R. A., J. L. Davis, and B. P. Wernicke (1999),
928 Present-day pattern of Cordilleran deformation in the western
929 United States, *Geology*, *27*, 371–374.
- 930 Blewitt, G. (2003), Self-consistency in reference frames, geo-
931 center definition, and surface loading of the solid Earth,
932 *J. Geophys. Res.*, *108*(B2), 2103, doi:10.1029/2002JB002082.
- 933 Brudzinski, M., E. Cabral-Cano, F. Correa-Mora, C. DeMets,
934 and B. Marquez-Azua (2007), Slow slip transients along the
935 Oaxaca subduction segment from 1993 to 2007, *Geophys. J. Int.*,
936 *171*, 523–538, doi:10.1111/j.1365-246X.2007.03542.x.
- 937 Calais, E., J. Y. Han, C. DeMets, and J. M. Nocquet (2006),
938 Deformation of the North American plate interior from a
939 decade of continuous GPS data, *J. Geophys. Res.*, *111*,
940 B06402, doi:10.1029/2005JB004253.
- 941 Correa-Mora, F., C. DeMets, E. Cabral-Cano, B. Marquez-
942 Azua, and O. Diaz-Molina (2008), Interplate coupling and
943 transient slip along the subduction interface beneath Oaxaca,
944 Mexico, *Geophys. J. Int.*, *175*, 269–290, doi:10.1111/j.1365-
945 246X.2008.03910.x.
- 946 DeMets, C. (1995), A reappraisal of seafloor spreading lineations
947 in the Gulf of California: Implications for the transfer of
948 Baja California to the Pacific plate and estimates of Pacific-
949 North America motion, *Geophys. Res. Lett.*, *22*, 3545–3548.
- 950 DeMets, C. (2001), A new estimate for present-day Cocos-
951 Caribbean plate motion: Implications for slip along the Central
952 American volcanic arc, *Geophys. Res. Lett.*, *28*, 4043–4046.
- 953 DeMets, C., and D. S. Wilson (1997), Relative motions of the
954 Pacific, Rivera, North American, and Cocos plates since
955 0.78 Ma, *J. Geophys. Res.*, *102*, 2789–2806.
- 956 Dixon, T., F. Farina, C. DeMets, F. Suarez Vidal, J. Fletcher,
957 B. Marquez-Azua, M. Miller, O. Sanchez, and P. Umhoefer
(2000), New kinematic models for Pacific-North America
958 motion from 3 Ma to present, II: Tectonic implications for Baja
959 and Alta California, *Geophys. Res. Lett.*, *27*, 3961–3964.
- 960 Ferrari, L., and J. Rosas-Elguera (2000), Late Miocene to
961 Quaternary extension at the northern boundary of the Jalisco
962 block, western Mexico: The Tepic-Zacoalco rift revised, in
963 *Cenozoic Tectonics and Volcanism of Mexico*, edited by
964 H. Delgado-Granados, G. Aguirre-Diaz, and J. Stock, *Geol.*
965 *Soc. Am. Spec. Pap.*, *334*, 41–64.
- 966 Franco, S. I., V. Kostoglodov, K. M. Larson, V. C. Manea,
967 M. Manea, and J. A. Santiago (2005), Propagation of the
968 2001–2002 silent earthquake and interplate coupling in the
969 Oaxaca subduction zone, Mexico, *Earth Planets Space*, *57*,
970 973–985.
- 971 Goff, J. A., E. A. Bergman, and S. C. Solomon (1987), Earth-
972 quake source mechanisms and transform fault tectonics in
973 the Gulf of California, *J. Geophys. Res.*, *92*, 10,485–10,510.
- 974 Guzman-Speziale, M., W. D. Pennington, and T. Matumoto
975 (1989), The triple junction of the North America, Cocos,
976 and Caribbean plates: Seismicity and tectonics, *Tectonophys-*
977 *ics*, *8*, 981–997.
- 978 Guzman-Speziale, M., and J. J. Meneses-Rocha (2000), The
979 North America-Caribbean plate boundary west of the
980 Motagua-Polochic fault system: a fault jog in southeastern
981 Mexico, *J. S. Am. Earth Sci.*, *13*, 459–468.
- 982 Heflin, M., et al. (1992), Global geodesy using GPS without
983 fiducial sites, *Geophys. Res. Lett.*, *19*, 131–134.
- 984 Hutton, W., C. DeMets, O. Sanchez, G. Suarez, and J. Stock
985 (2001), Slip kinematics and dynamics during and after
986 the 1995 October 9 $M_w = 8.0$ Colima-Jalisco earthquake,
987 Mexico, from GPS geodetic constraints, *Geophys. J. Inter.*,
988 *146*, 637–658.
- 989 Kostoglodov, V., S. K. Singh, J. A. Santiago, S. I. Franco,
990 K. M. Larson, A. R. Lowry, and R. Bilham (2003), A large
991 silent earthquake in the Guerrero seismic gap, Mexico, *Geo-*
992 *phys. Res. Lett.*, *30*(15), 1807, doi:10.1029/2003GL017219.
- 993 Langbein, J. (2008), Noise in GPS displacement measurements
994 from southern California and southern Nevada, *J. Geophys.*
995 *Res.*, *113*, B05405, doi:10.1029/2007JB005247.
- 996 Langridge, R. M., R. J. Weldon II, J. C. Moya, and G. Suarez
997 (2000), Paleoseismology of the 1912 Acambay earthquake
998 and the Acambay-Tixmadeje fault, Trans-Mexican Volcanic
999 Belt, *J. Geophys. Res.*, *105*, 3019–3037.
- 1000 Larson, K. M., A. R. Lowry, V. Kostoglodov, W. Hutton,
1001 O. Sanchez, K. Hudnut, and G. Suarez (2004), Crustal
1002 deformation measurements in Guerrero, Mexico, *J. Geo-*
1003 *phys. Res.*, *109*, B04409, doi:10.1029/2003JB002843.
- 1004 Larson, K. M., V. Kostoglodov, S. Miyazaki, and J. A. S.
1005 Santiago (2007), The 2006 aseismic slow slip event in Guer-
1006 rero, Mexico: New results from GPS, *Geophys. Res. Lett.*,
1007 *34*, L13309, doi:10.1029/2007GL029912.
- 1008 Lowry, A., K. Larson, V. Kostoglodov, and R. Bilham (2001),
1009 Transient fault slip in Guerrero, southern Mexico, *Geophys.*
1010 *Res. Lett.*, *28*, 3753–3756.
- 1011 Mao, A., C. G. A. Harrison, and T. H. Dixon (1999), Noise
1012 in GPS coordinate time series, *J. Geophys. Res.*, *104*,
1013 2797–2816.
- 1014 Marquez-Azua, B., and C. DeMets (2003), Crustal velocity field
1015 of Mexico from continuous GPS measurements, 1993 to June,
1016 2001: Implications for the neotectonics of Mexico, *J. Geo-*
1017 *phys. Res.*, *108*(B9), 2450, doi:10.1029/2002JB002241.
- 1018 Marquez-Azua, B., C. DeMets, and T. Masterlark (2002), Strong
1019 interseismic coupling, fault afterslip, and viscoelastic flow be-
1020 fore and after the Oct. 9, 1995 Colima-Jalisco earthquake: Con-
1021 tinuous GPS measurements from Colima, Mexico, *Geophys.*
1022 *Res. Lett.*, *29*(8), 1281, doi:10.1029/2002GL014702.
- 1023



- 1024 Marquez-Azua, B., E. Cabral-Cano, F. Correa-Mora, and
1025 C. DeMets (2004), A model for Mexican neotectonics based
1026 on nationwide GPS measurements, 1993–2001, *Geof. Int.*,
1027 43, 319–330.
- 1028 Melbourne, T., I. Carmichael, C. DeMets, K. Hudnut, O. Sanchez,
1029 J. Stock, G. Suarez, and F. Webb (1997), The geodetic signature
1030 of the M8.0 October 9, 1995, Jalisco subduction earthquake,
1031 *Geophys. Res. Lett.*, 24, 715–718.
- 1032 Mendoza, C., and S. Hartzell (1999), Fault-slip distribution of
1033 the 1995 Colima-Jalisco, Mexico, earthquake, *Bull. Seismol.*
1034 *Soc. Am.*, 89, 1338–1344.
- 1035 Michaud, F., et al. (2004), Motion partitioning between the
1036 Pacific plate, Baja California, and the North America plate:
1037 The Tosco-Abreojos fault revisited, *Geophys. Res. Lett.*, 31,
1038 L08604, doi:10.1029/2004GL019665.
- 1039 Plattner, C., R. Malservisi, T. H. Dixon, P. LaFemina, G. Sella,
1040 J. Fletcher, and F. Vidal-Suarez (2007), New constraints on
1041 relative motion between the Pacific plate and Baja California
1042 microplate (Mexico) from GPS measurements, *Geophys. J. Int.*,
1043 170, 1373–1380, doi:10.1111/j.1365-246X.2007.03494.x.
- 1044 Schmitt, S. V., C. DeMets, J. Stock, O. Sanchez, B. Marquez-
1045 Azua, and G. Reyes (2007), A geodetic study of the 2003 Jan-
1046 uary 22 Tecoman, Colima, Mexico earthquake, *Geophys. J. Int.*,
1047 169, 389–406, doi:10.1111/j.1365-246X.2006.03322.x.
- 1048 Sella, G. F., S. Stein, T. H. Dixon, M. Craymer, S. James,
1049 S. Mazzotti, and R. K. Dokka (2007), Observation of glacial
isostatic adjustment in “stable” North America with GPS, 1050
Geophys. Res. Lett., 34, L02306, doi:10.1029/2006GL027081. 1051
- Suarez, G., and O. Sanchez (1996), Shallow depth of seismo- 1052
genic coupling in southern Mexico: Implications for the 1053
maximum size of earthquakes in the subduction zone, *Phys.* 1054
Earth Planet. Int., 93, 53–61. 1055
- Suter, M., M. López Martínez, O. Quintero Legorreta, and 1056
M. Carrillo Martínez (2001), Quaternary intra-arc extension 1057
in the central Trans-Mexican volcanic belt, *Geol. Soc. Am.* 1058
Bull., 113, 693–703. 1059
- Ward, S. N. (1990), Pacific-North America plate motions: New 1060
results from very long baseline interferometry, *J. Geophys.* 1061
Res., 95, 21,965–21,981. 1062
- Williams, S. D. P., Y. Bock, P. Fang, P. Jamason, R. M. 1063
Nikolaidis, L. Prawirodirdjo, M. Miller, and D. J. Johnson 1064
(2004), Error analysis of continuous GPS time series, *J. Geo-* 1065
phys. Res., 109, B03412, doi:10.1029/2003JB002741. 1066
- Yoshioka, S., T. Mikumo, V. Kostoglodov, K. M. Larson, A. R. 1067
Lowry, and S. K. Singh (2004), Interplate coupling and a 1068
recent aseismic slow slip event in the Guerrero seismic gap 1069
of the Mexican subduction zone, as deduced from GPS data 1070
inversion using a Bayesian information criterion, *Phys.* 1071
Earth Planet. Inter., 146, 513–530. 1072
- Zumberge, J. F., M. B. Heflin, D. C. Jefferson, M. M. Watkins, 1073
and F. H. Webb (1997), Precise point positioning for the 1074
efficient and robust analysis of GPS data from large net- 1075
works, *J. Geophys. Res.*, 102, 5005–5017. 1076

Article in Press